Coding Cross Sections of an Electron Charge Transfer Process: Analysis of Different Cuts for the Entrance and Exit Potentials

Noelia Faginas-Lago[1(✉)], Emília Valença Ferreira de Aragão[1,2], Luca Mancini[1], Marzio Rosi[4], Daniela Ascenzi[3], and Fernando Pirani[1,4]

[1] Dipartimento di Chimica, Biologia e Biotecnologie, Università degli Studi di Perugia, 06123 Perugia, Italy
{emilia.dearagao,luca.mancini2}@studenti.unipg.it,
{noelia.faginaslago,fernando.pirani}@unipg.it
[2] Master-tec srl, Via Sicilia 41, 06128 Perugia, Italy
emilia.dearagao@master-tec.it
[3] Dipartimento di Fisica, Università di Trento, Trento, Italy
daniela.ascenzi@unitn.it
[4] Dipartimento di Ingegneria Civile ed Ambientale, Università degli Studi di Perugia, 06125 Perugia, Italy
marzio.rosi@unipg.it

Abstract. The paper presents the algorithm of a code written for exploring the collision dynamics of an electron transfer process between a neutral species and helium cation. Cuts of the entrance and exit potential energy surfaces are calculated in function of the radial distance to the center of mass of the neutral molecule, inclination angle and azimuth. Entrance and exit potential are calculated accounting for the electrostatic contribution and for non-electrostatic forces by employing the Improved Lennard-Jones function.

The code implemented has been employed in systems involving helium cation and a small organic molecule, such as methanol, dimethyl ether and methyl formate.

Keywords: Astrochemistry · Semiempirical potential · Improved Lennard-Jones · Charge exchange process

1 Introduction

Among more than 289 molecular species detected in the interstellar and circumstellar medium [1–4], particular interest is directed to the so called interstellar Complex Organic Molecules (iCOMS), namely organic molecules containing at least six atoms, including heavier element such as nitrogen and/or oxygen [5,6]. The detection of relatively complex and prebiotic molecules in the harsh regions of the interstellar medium (where the temperature can go down to 10 K and the

© The Author(s), under exclusive license to Springer Nature Switzerland AG 2023
O. Gervasi et al. (Eds.): ICCSA 2023 Workshops, LNCS 14111, pp. 162–175, 2023.
https://doi.org/10.1007/978-3-031-37126-4_12

particle density can be as low as 10^4 particles cm^{-3} [7]), led to an increased interest in our understanding of interstellar chemistry. In order to properly describe the chemical complexity of the interstellar medium (ISM), different astrochemical models have been developed [8–13]. In particular, a multidisciplinary approach appears to be pivotal, combining data coming from astronomical observations as well as chemical and physical investigations. At the present stage, in order to explain the abundances of interstellar molecules, a synergy between two main reaction mechanism, namely grain surface processes and gas-phase reactions, must be invoked. The only use of grain surface chemistry (according to which iCOMs are initially formed through hydrogenation and radical recombination processes on the surface of the grains and subsequently ejected in the gas phase [7]) does not allow to reproduce the detected abundances. Therefore, a combined approach including gas-phase reactions is crucial for a correct implementation of astrochemical models, as pointed out by recent works [14–16]. Considering the prohibitive conditions of the interstellar medium, only barrierless and exothermic process appears to be feasible chemical routes in the gas phase, namely reaction between ions and/or radicals with closed-shell species. An accurate characterization of chemical reactions (both with theoretical calculation and experimental investigations) is indeed pivotal to derive the parameters used in the astrochemical models. An example of the aforementioned models is represented by the two KIDA [17] and UMIST [18] databases, in which the abundances of detected species are accounted for by considering their formation and destruction routes. Unfortunately, among the 8000 reactions considered, only a small fraction is derived through accurate chemical analysis, while the remaining part is included with estimated parameters considered on the basis of chemical analogies. As already mentioned, together with the possible formation mechanisms, also destruction routes play an extremely important role for the global astrochemical modeling. The main destruction processes for iCOMs in the gas phase are driven by ions, namely He^+ or H_3^+ and HCO^+. Among this species, He^+ represents one of the best candidate [19,20], due to its high value of ionisation energy [21], leading to a charge transfer process followed by the dissociation of the new-formed ion. The dynamics of the charge transfer processes is driven by the probability of the transition between different intermolecular Potential Energy Surfaces (PESs), which depends on the orientation of the interacting fragments. In the present contribution, we describe a code developed by our group in order to calculate the cross sections for the global electron transfer process, to be compared with results measured as a function of the collision energy with the molecular beam technique, and, subsequently, to evaluate related reaction rate constants as a function of the temperature.

2 Program Implementation

The code has been developed to compute cuts of entrance and exit potential energy surfaces for the charge exchange process. The cuts are calculated in function of the spherical coordinates of He^+ and He for the entrance and exit PESs,

respectively. The goal is to identify the configurations where an exothermic crossing between the two PESs can be observed. The code was written in C language, and has the following structure:

1. Inclusion of useful libraries as stdio.h, math.h, stdlib.h and string.h;
2. Definition of assorted functions;
3. Main program section, defined inside "*int main*{...}".

In the next sections, a detailed description of the contents of each piece of code is given.

2.1 Definition of Assorted Functions

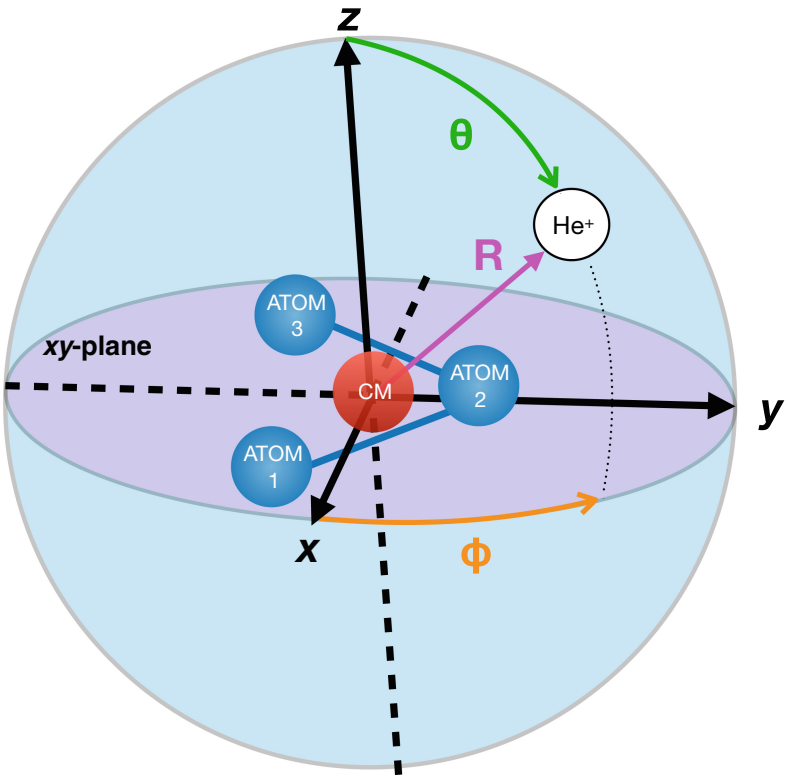

Fig. 1. Scheme representing a system in a three-dimensional space. The molecule is represented by its effective atoms, in blue, and by its center of mass (CM), in red, which is used as the origin of the Cartesian reference system. In the code, the position of He^+ is declared in terms of spherical coordinates, with R being the distance between the molecule's CM and the ion, θ being the angle made by the R vector with the z-axis and ϕ defined as the azimuthal angle.

The functions implemented here are similar to what was described in a previous work by our group [22]. They involve the definition of the frame of reference and the definition of the entrance and exit potentials functions. As in our previous work, what we call "configuration" here is an individual relative spatial orientation between the neutral molecule (e.g. dimethyl ether, methyl formate, methanol) and He^+.

Before using the code, the user must obtain the optimized geometry of the molecule and the partial atomic charges via quantum chemistry calculations employing *ab initio* methods. In case of molecules containing many atoms, it is recommended to replace functional groups with effective atoms, for instance C_{eff} instead of a methyl group. Here, C_{eff} has the mass and the polarizability of a methyl group. The partition of the molecular polarizability in functional group components has been successfully adopted to build up the force field useful in several molecular dynamics simulations (see, for instance, [23,24]) Moreover, for the molecules of interest in this study, the partial charge of the effective atom will be the sum of the partial charges of all the atoms it is representing. The center of mass (CM) of the molecule, shown in red in 1, is defined via the equations:

$$x_{CM} = \frac{\sum_{i=1}^{N} x_i m_i}{M};\ y_{CM} = \frac{\sum_{i=1}^{N} y_i m_i}{M};\ z_{CM} = \frac{\sum_{i=1}^{N} z_i m_i}{M} \tag{1}$$

where x_i, y_i and z_i are the coordinates of each effective atom, m_i its mass, N the total number of effective atoms and M the total mass of the molecule. A new Cartesian frame of reference must be defined, with CM placed at its origin, in order to make the declaration of the position of the ion easier later. The coordinates of the effective atoms in this new frame of reference, are obtained by extracting the CM coordinates from the original atomic coordinates:

$$x_i' = x_i - x_{CM};\ y_i' = y_i - y_{CM};\ z_i' = z_i - z_{CM} \tag{2}$$

As for He^+, the user must give the value of the spherical coordinates and the program will compute the Cartesian coordinates (denoted by j) using the following formulae:

$$x_j = Rsin(\theta)cos(\phi) \tag{3}$$

$$y_j = Rsin(\theta)sin(\phi) \tag{4}$$

$$z_j = Rcos(\theta) \tag{5}$$

where R is the distance between the ion and the CM, θ the angle in relation with the z-axis and ϕ is the azimuth angle. R values can range from 0 to infinite, θ values range from 0° to 180° and ϕ ranges from 0° to 360°. For a molecule with a certain degree of symmetry, the user can choose to explore a reduced range of values for θ and ϕ.

As shown in Fig. 2, the potential functions are dependent of the distance between each effective atom of the molecule and the ion, r_{ij}, which can be calculated as follows:

$$r_{ij} = \sqrt{(x_i - x_j)^2 + (y_i - y_j)^2 + (z_i - z_j)^2} \tag{6}$$

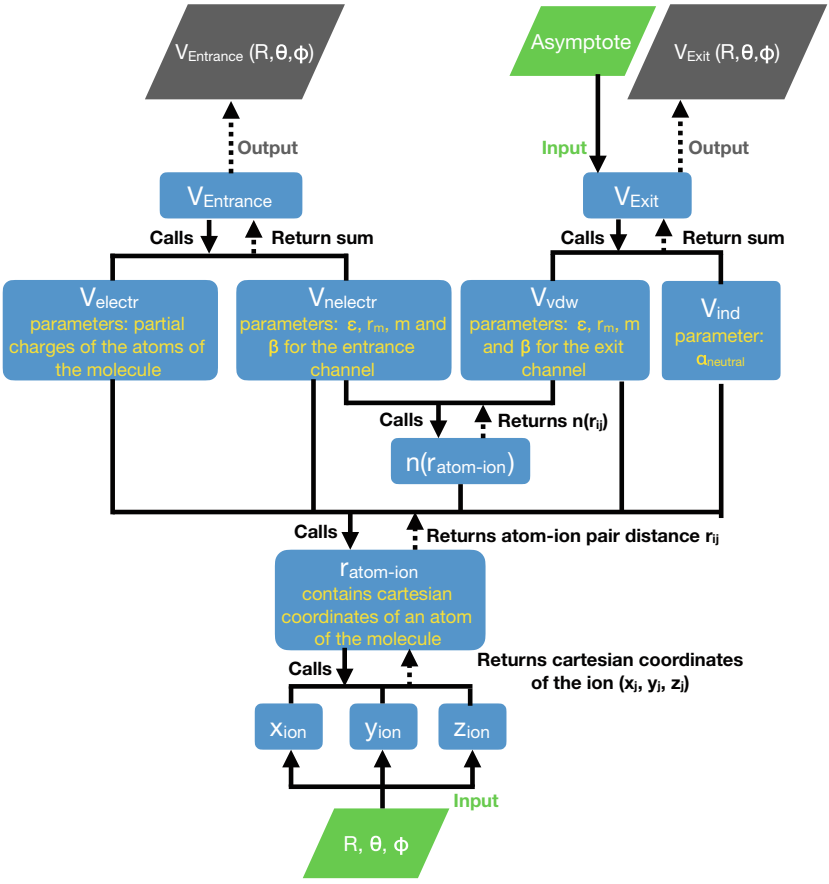

Fig. 2. An overall view of the algorithm in *pes.c* code. In green, the input information, in grey the output. Blue blocks refer to functions that have been defined outside the main section of the program.

The potential functions must also be adapted to each system, and so the definition of some parameters are necessary before using the program. For instance, the partial charges on the neutral species obtained through *ab initio* calculations are used to estimate the electrostatic contribution for the entrance PES, $V_{electr}(R)$. In the case of the non-electrostatic contribution, represented by the sum of individual V_{ij} (again, i represents an atom of the molecule and j denotes He^+), a handful of parameters must be adopted. These parameters are the potential well ε_{ij} and the related equilibrium distance $r_{m_{ij}}$, whose values are used to evaluate V_{ij} through the Improved Lennard-Jones model [25]:

$$V_{ij}(r_{ij}) = \varepsilon_{ij}\left[\frac{m}{n(r_{ij})-m}\left(\frac{r_{m_{ij}}}{r_{ij}}\right)^{n(r_{ij})} - \frac{n(r_{ij})}{n(r_{ij})-m}\left(\frac{r_{m_{ij}}}{r_{ij}}\right)^{m}\right] \tag{7}$$

where m, as explained in [25,26], is parameter depending on the nature of the system: it assumes the value of 1 for ion-ion interaction, 2 for ion-permanent dipole, 4 for ion-induced dipole, and 6 for neutral-neutral pairs. In the present case, since the entrance channel involves a small ion and a neutral molecule, the induction attraction dominates over the dispersion, and so $m = 4$ is assumed. After the charge transfer process, we have a molecular ion interacting with an atom with low polarizability, so the dispersion plays a more important role and m assumes the value of 6. The modulation in the decline of the repulsion and the enhancement of the attraction in Eq. 7, $n(r_{ij})$ takes the following form:

$$n(r_{ij}) = \beta + 4\left(\frac{r_{ij}}{r_{m_{ij}}}\right)^2 \tag{8}$$

where β is a parameter related to the nature and the hardness of the interacting particles [26–29] and the $\frac{r_{ij}}{r_{m_{ij}}}$ ratio is introduced as a reduced distance. The total non-electrostatic contribution, which is the sum of all V_{ij} of a given configuration, is called $V_{nelectr}$ in the entrance channel and V_{vdw} in the exit channel (see Fig. 2).

In the entrance channel, the electrostatic component $V_{electr}(R)$ is defined by the Coulomb's law:

$$V_{\text{electr}}(R) = \frac{1}{4\pi\varepsilon_0}\sum_{i}^{N}\frac{q_i}{r_{ij}} \tag{9}$$

where R is again the distance between the ion and CM, r_{ij} is again the distance between an atom of the molecule and the ion, obtained deconvolving R into partial components, ε_0 is the vacuum permittivity, and q_i corresponds to the partial charge on each atom of the molecule.

In the exit channel, an induction term is inserted to represent the ion-induced dipole contribution as a pertubative approach. The induction term, $V_{ind}(R')$, describes the interaction between the newly formed molecular cation and He. Considering the polarizability $\alpha_{neutral}$ of the He, $V_{ind}(R')$ is expressed adopting the following formalism:

$$V_{ind}(R') = -7200\frac{\alpha_{neutral}}{R'^4} \tag{10}$$

By analogy to R, R' is the distance between the neutralized species and the center-of-mass of the newly formed cation. In our code, we assume $R = R'$ whenever we want to explore a crossing between the entrance and the exit channels.

Our code requires one parameter for the exit channel, the so called asymptote. The asymptote is calculated by taking the first ionization energy value of Helium and subtracting the ionization energy of the molecular orbital from which the electron is being extracted. This allows the user to estimate from which orbital(s) of the molecule the electron might be removed during the charge transfer process. The difference between the two energies must be taken into account when defining the exit PES in order to see if the cuts of the entrance and exit PESs are crossing each other at some point. Figure 2 shows the algorithm of the

pes.c code. In green are represented the input information, such as the spherical coordinates of the ion and the asymptote. In blue are reported the functions code in the program, implemented with the equations previously reported. The outputs, represented in grey, contain the values of the entrance and exit potentials for a given configuration. With this program, it is possible to have different cuts of the entrance and exit PESs, and so it is possible to visualise in which configurations the crossing might happen. In the next sections, we will briefly talk about the options of routine in the code that produce different outputs.

2.2 Calculating the PESs Curves in Function of R

The previous section described all the functions that have been implemented in the code. This section provides an explanation on how the program calculates the entrance and exit potential in function of R, as depicted in Fig. 3.

First, in the user must declare the value of the inclination (θ), azimuth (ϕ), frozen distance (d) and asymptote inside the program. θ, ϕ must be declared in radians, d in angstroms and the asymptote must be in eV. Then the program will open two empty output files, one for the entrance potential and one for the exit potential. A loop will start by setting the value of R to 1.0 (in angstroms) and it will run until R = 12.0 Å by increasing the value of R with 0.001 Å at each step. Of course, these values may be modified according to the user needs. Inside the loop, the code will call for the function $V_{Entrance}$, which will in turn call a succession of other functions (see Fig. 2). Then the code will write a line in the output file 1 the values of R, $V_{Entrance}(R)$ $(= V_{Entrance}(R, \theta, \phi))$ and the respective electrostatic and non-electrostatic components of $V_{Entrance}(R)$. Output file 1 should have 4 columns is total. Next, the code calls for the function V_{Exit}, which like $V_{Entrance}$ will call for many other functions. It will write in output file 2 a line with the values of R, $V_{Exit}(R)$ $(= V_{Exit}(R, \theta, \phi))$ and the respective non-electrostatic contribution and induction contribution.

Once the loop ends, the program will open a third output file in *.xyz* format. It will also open and read a file called "molecule.xyz", which should contain the total number of atoms in the molecule and their respective Cartesian coordinates. Next, the program will attribute a value to the frozen distance d, for instance 3.5 Å. The Cartesian coordinates of He^+ will then be computed for a configuration where He^+ is 3.5 Å away from the center of mass of the molecule. The program will write in output file 3 in .xyz and write the total number of atoms of the complex, the Cartesian coordinates of the atoms of the molecule and the Cartesian coordinates of He^+. Finally, the program will close the output files and stop.

The purpose of output file 3 is to help the user visualize the relative orientation of He^+ and the molecule for a specific pair of θ and ϕ. This file can be open with a molecular visualization software such as Avogadro [30]. Output files 1 and 2, on the other hand, can be read by any software for data analysis. The user can ask the software, for instance, to plot the entrance and exit PESs curves together in order to observe the presence of an exothermic crossing or to

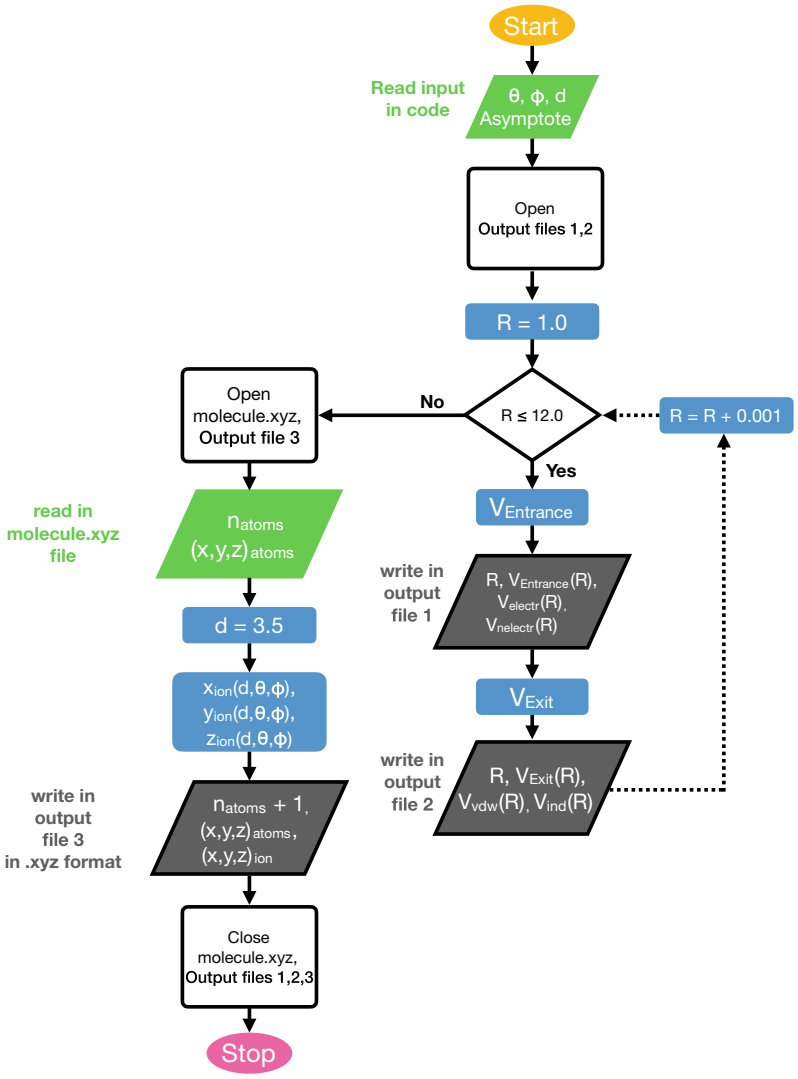

Fig. 3. Flowchart showing how the program operates for the calculation of the entrance and exit potential in function of the distance R. R is assumed as the distance between He^+ and the center of mass of the molecule as well as the distance between He and the center of mass of the molecular cation.

analyse the effects of the electrostatic and non-electrostatic contributions in the total potential.

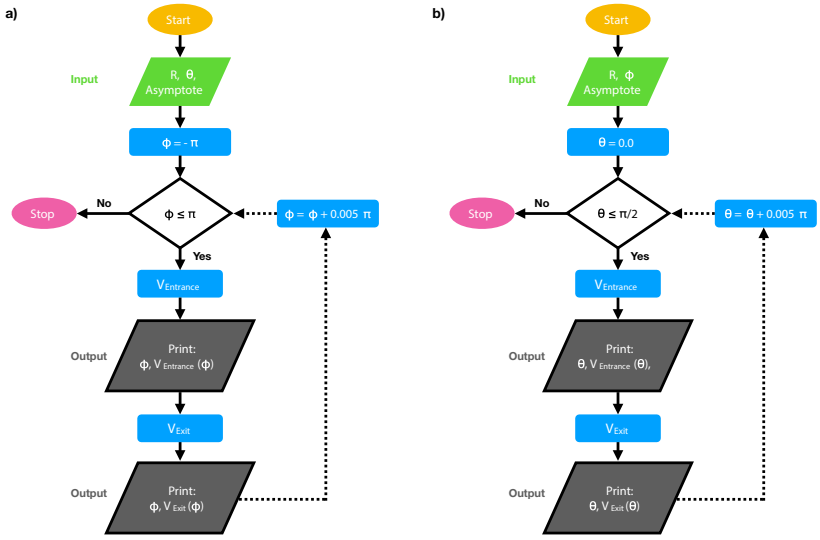

Fig. 4. Flowchart showing how the program operates for the calculation of the entrance and exit potential in function of the azimuth ϕ (a) and the inclination angle θ (b).

2.3 Calculating the PESs Curves in Function of θ and ϕ

The routines in this program are similar to the previous one, but instead the user can use it to explore the cuts of the entrance and exit PESs in function of the azimuth ϕ (Fig. 4a) and the inclination angle θ (Fig. 4b). The routine starts by reading a fixed value of R, the asymptote and θ (or ϕ). Then the value of ϕ (or θ) is set to a minimal value. In principle, for the loop in Fig. 4a, one can calculate the potential for any value of $-\pi \leq \phi \leq \pi$. If the molecule presents a certain degree of symmetry, the values of the loop can be reduced to $0 \leq \phi \leq \pi$ at the user's discretion. The same can be done in Fig. 4b in respect to the values of θ, which in principle range from $-\frac{\pi}{2}$ to $\frac{\pi}{2}$, but in the image is shown from 0 to $\frac{\pi}{2}$.

Inside the loop in Fig. 4a, the output files should contain two columns, one for ϕ and another for the $V_{Entrance}$ (or the V_{Exit}) in function of (R,θ,ϕ). As input values, the user can add columns in the previous file to be able to calculate the potential at different values of R (2 Å, 10 Å, 15 Å, etc.), in order to have an idea of the long range behaviour of the potential observed at different values of the azimuth. Again, this also applies to the routine in Fig. 4b.

The user can open the output files with any software that plots graphs. The plot will show the behaviour of the entrance and exit potentials at a given distance R between the two chemical species for many angles of attack.

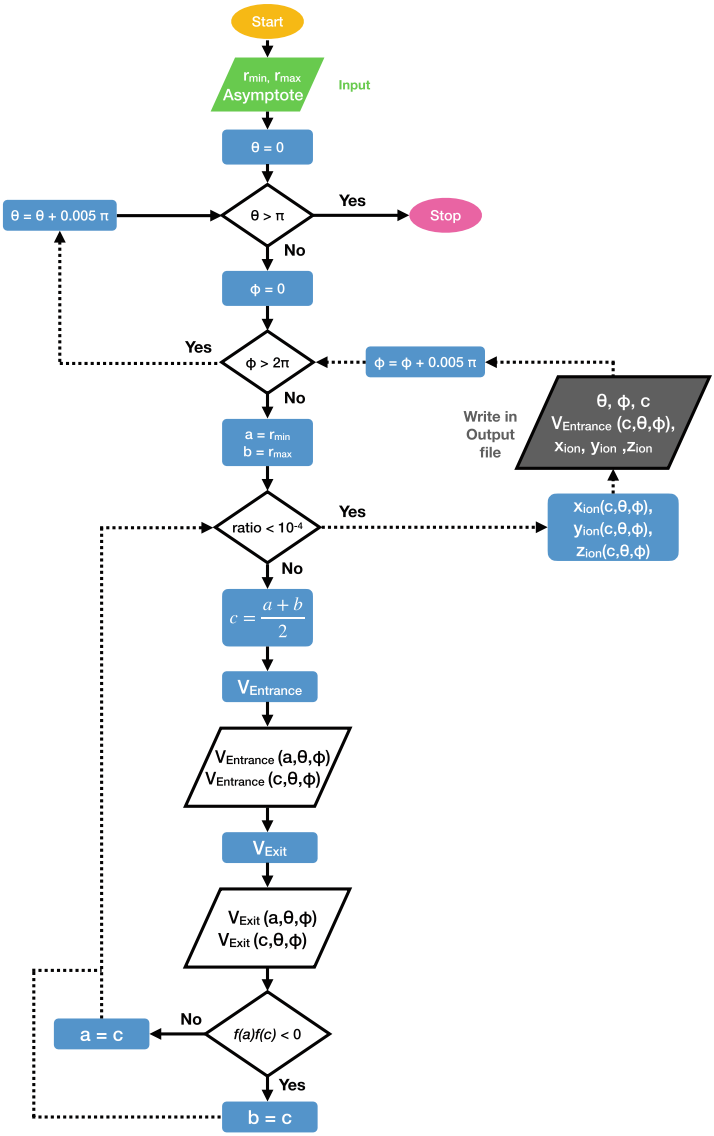

Fig. 5. Flowchart showing the process of finding the crossing point for several configurations.

2.4 Mapping the Crossing Points

In this section we present a new feature of our code. In fact, one of the goals of the analysis of the entrance and exit PESs cuts is to find the configurations in which an exothermic crossing is possible. We found it could be interesting to have a way to visualize the regions surrounding the molecule where the crossing

can happen. For that, we created a routine in the code that will go through several configurations (θ and ϕ pairs) around the molecule and try to find if crossing is possible and at what distance from the CM it will happen.

First, the user must declare the value of the asymptote and r_{min} and r_{max} which are, respectively, the minimum and maximum values of the distance where the crossing point might be located. They have to be adapted by the user for the system of interest. From this point on, the program will enter a series of three loops.

The outermost loop starts after setting the value of θ to 0 and it will run by increasing the value of theta θ by 0.005 π until $\theta > \pi$. This corresponds to 201 individual values of θ. The second outermost loop is entered after the value of the azimuth is set to 0 as well and it runs until $\theta > 2\pi$, with the increment of 0.005 π at each turn. Therefore, the program runs for about 401 different values of ϕ. In total, the program evaluates the possibility of crossing points in 80.601 different configurations and for a molecule with 3 effective atoms it takes around 28 s.

Inside that second loop, *i.e* for a given configuration, two variables called a and b are set with the values of r_{min} and r_{max}, respectively. At this point the program starts a routine to find the value of the distance where the entrance and exit potential curves intersect. This is done by means of the well known bisection method, an iterative method that consists in updating the value of the distance (here c), until the root of the function of interest is found. Lets call the function of interest $f(x)$, defined as:

$$f(x) = V_{Entrance}(x, \theta, \phi) - V_{Exit}(x, \theta, \phi) \tag{11}$$

By entering the innermost loop of our program, the value of c is set as the midpoint of [a;b] interval:

$$c = \frac{a+b}{2} \tag{12}$$

The program calls the function $V_{Entrance}$ to compute $V_{Entrance}(a, \theta, \phi)$ and $V_{Entrance}(c, \theta, \phi)$ and then it calls the function V_{Exit} to compute $V_{Exit}(a, \theta, \phi)$ and $V_{Exit}(c, \theta, \phi)$. With this information, $f(a)$ and $f(c)$ are calculated using the formula in Eq. 11. The need to readjust either the value of a or b is then evaluated by observing the sign of the product of $f(a)f(c)$. If $f(a)f(c) < 0$, that means that the function $f(x)$ went through a sign change between a and c. In other words, the root of $f(x)$ is somewhere between a and c, but not between c and b. So b value is updated to take the value of c. On the contrary, if $f(a)f(c) < 0$, then a takes the value of c instead. The program stays in the innermost loop until it fulfils the following condition:

$$\left| \frac{a-b}{a+b} \right| < 10^{-4} \tag{13}$$

In Fig 5, $\frac{a-b}{a+b}$ is represented by "ratio". At this point, the value of c should give the location of the crossing point. The Cartesian coordinates of He+ are computed and then a line in the output file is printed with θ, ϕ, c, the value

of the entrance potential at this configuration, and the Cartesian coordinates of He^+. The program stops when it fulfils the condition $\theta > \pi$.

The generated output file should have more than 80.000 lines, each corresponding to a configuration. In some of them, the value of c is close to r_{max}, and in this case it is probable that there is not a crossing point for that configuration. In other cases, the value of c will be somewhere between the r_{min} and r_{max}, but the value of the potential will be positive, which means that the crossing point is endothermic. Alternatively, the user might chose to ask the code to write in the output only the configurations where the crossing is exothermic. Then, the user can use a program to make a 3D scattering plot containing the Cartesian coordinates of Helium. In the same graph, the user can plot the Cartesian coordinates of the molecule. This will give the user an overall view of the configurations around the molecule where the exothermic crossing is possible.

3 Conclusions

The piece of code described has been used in four systems so far, all of them involving He^+ colliding with dimethyl ether [31], methyl formate [32], methanol [33] and acetonitrile (under study) . The results of these codes are very important as they are the preliminary step before calculating the total cross section, as detailed in [22]. Compared to [22], more time has been dedicated to explore the PESs cuts as a function of the angle θ and azimuth ϕ. In addition, a new routine was implemented to generate a file where the user can see in 3D the regions surrounding the molecule where the crossing can happen. This will be helpful when the user later defines the set of preferential orientations to compute the cross section, as done in [33].

Acknowledgements. The authors thank Andrea Cernuto who originally developed the code. This project has received funding from the European Union's Horizon 2020 research and innovation programme under the Marie Skłodowska Curie grant agreement No 811312 for the project "Astro-Chemical Origins" (ACO).

The authors thank the Herla Project(http://www.hpc.unipg.it/hosting/vherla/vherla.html)-Università degli Studi di Perugia for allocated computing time.

N.F-L acknowledges also Fondazione Cassa di Risparmio di Perugia n 19839_2020_0513 to C.E.

D.A. and M.R. acknowledge funding from MUR PRIN 2020 project n. 2020AF B3FX.

References

1. McGuire, B.A.: 2021 census of interstellar, circumstellar, extragalactic, protoplanetary disk, and exoplanetary molecules. Astrophys. J. Suppl. Ser. **259**(2), 30 (2022). https://doi.org/10.3847/1538-4365/ac2a48
2. Müller, H.S.P., Thorwirth, S., Roth, D.A., Winnewisser, G.: The cologne database for molecular spectroscopy, CDMS. A& A **370**(3), L49–L52 (2001). https://doi.org/10.1051/0004-6361:20010367. https://cdms.astro.uni-koeln.de/classic/molecules. Accessed 13 April 2022

3. Müller, H.S., Schlöder, F., Stutzki, J., Winnewisser, G.: The cologne database for molecular spectroscopy, CDMS: a useful tool for astronomers and spectroscopists. J. Mol. Struct. **742**(1), 215–227 (2005). https://doi.org/10.1016/j.molstruc.2005.01.027
4. Endres, C.P., Schlemmer, S., Schilke, P., Stutzki, J., Müller, H.S.: The cologne database for molecular spectroscopy, CDMS, In the virtual atomic and molecular data centre, VAMDC. J. Molecular Spectroscopy **327**, 95–104 (2016). https://doi.org/10.1016/j.jms.2016.03.005. New Visions of Spectroscopic Databases, Volume II
5. Herbst, E., Van Dishoeck, E.F.: Complex organic interstellar molecules. Ann. Rev. Astron. Astrophys. **47**, 427–480 (2009)
6. Ceccarelli, C., et al.: Seeds of life in space (SOLIS): the organic composition diversity at 300–1000 au scale in solar-type star-forming regions. Astrophys. J. **850**(2), 176 (2017)
7. Caselli, P., Ceccarelli, C.: Our astrochemical heritage. Astron. Astrophys. Rev. **20**(1), 1–68 (2012). https://doi.org/10.1007/s00159-012-0056-x
8. Herbst, E.: The synthesis of large interstellar molecules. Int. Rev. Phys. Chem. **36**(2), 287–331 (2017)
9. Agúndez, M., Wakelam, V.: Chemistry of dark clouds: databases, networks, and models. Chem. Rev. **113**(12), 8710–8737 (2013)
10. Taquet, V., Ceccarelli, C., Kahane, C.: Multilayer modeling of porous grain surface chemistry-I. GRAINOBLE Model. Astron. Astrophys. **538**, A42 (2012)
11. Garrod, R., Herbst, E.: Formation of methyl formate and other organic species in the warm-up phase of hot molecular cores. Astron. Astrophys. **457**(3), 927–936 (2006)
12. Vasyunin, A.I., Caselli, P., Dulieu, F., Jiménez-Serra, I.: Formation of complex molecules in prestellar cores: a multilayer approach. Astrophys. J. **842**(1), 33 (2017)
13. Garrod, R.T., Weaver, S.L.W., Herbst, E.: Complex chemistry in star-forming regions: an expanded gas-grain warm-up chemical model. Astrophys. J. **682**(1), 283 (2008)
14. Balucani, N., Ceccarelli, C., Taquet, V.: Formation of complex organic molecules in cold objects: the role of gas-phase reactions. Monthly Notices Royal Astron. Soc.: Lett. **449**(1), L16–L20 (2015)
15. Skouteris, D., et al.: The genealogical tree of ethanol: gas-phase formation of glycolaldehyde, acetic acid, and formic acid. Astrophys. J. **854**(2), 135 (2018)
16. Rosi, M., et al.: Possible scenarios for SiS formation in the interstellar medium: Electronic structure calculations of the potential energy surfaces for the reactions of the SiH radical with atomic sulphur and S_2. Chem. Phys. Lett. **695**, 87–93 (2018). https://doi.org/10.1016/j.cplett.2018.01.053
17. Wakelam, V., et al.: A kinetic database for astrochemistry (KIDA). ApJS **199**(1), 21 (2012). https://doi.org/10.1088/0067-0049/199/1/21
18. Woodall, J., Agúndez, M., Markwick-Kemper, A.J., Millar, T.J.: The UMIST database for astrochemistry 2006*. A&A **466**(3), 1197–1204 (2007). https://doi.org/10.1051/0004-6361:20064981
19. Lepp, S., Stancil, P., Dalgarno, A.: Atomic and molecular processes in the early Universe. J. Phys. B: At. Mol. Opt. Phys. **35**(10), R57 (2002)
20. De Fazio, D.: The H + $HeH^+ \rightarrow He^+$ H_2^+ reaction from the ultra-cold regime to the three-body breakup: exact quantum mechanical integral cross sections and rate constants. Phys. Chem. Chem. Phys. **16**(23), 11662–11672 (2014). https://doi.org/10.1039/C4CP00502C

21. Mallard, W., Linstrom, P.: NIST Chemistry WebBook, NIST Standard Reference Database Number 69. Gaithersburg, MD 20899 (2000). https://doi.org/10.18434/T4D303
22. de Aragão, E.V.F., et al.: Coding cross sections of an electron charge transfer process. In: Gervasi, O., Murgante, B., Misra, S., Rocha, A.M.A.C., Garau, C. (eds.) Computational Science and Its Applications - ICCSA 2022 Workshops. ICCSA 2022. Lecture Notes in Computer Science, vol. 13382, pp. 319–333. Springer, Cham (2022). https://doi.org/10.1007/978-3-031-10592-0_24
23. Albertí, M., Faginas-Lago, N., Laganà, A., Pirani, F.: Phys. Chem. Chem. Phys. **13**(18), 8422 (2011)
24. Faginas Lago, N., Albertí, M., Lombardi, A., Pirani, F.: A force field for acetone: the transition from small clusters to liquid phase investigated by molecular dynamics simulations. Theoret. Chem. Acc. **135**(7), 1–9 (2016). https://doi.org/10.1007/s00214-016-1914-9
25. Pirani, F., Brizi, S., Roncaratti, L.F., Casavecchia, P., Cappelletti, D., Vecchiocattivi, F.: Beyond the Lennard-Jones model: a simple and accurate potential function probed by high resolution scattering data useful for molecular dynamics simulations. Phys. Chem. Chem. Phys. **10**(36), 5489–5503 (2008)
26. Pirani, F., Albertí, M., Castro, A., Moix Teixidor, M., Cappelletti, D.: Atom-bond pairwise additive representation for intermolecular potential energy surfaces. Chem. Phys. Lett. **394**(1–3), 37–44 (2004). https://doi.org/10.1016/j.cplett.2004.06.100
27. Bartolomei, M., et al.: The intermolecular potential in NO-N_2 and $(NO\text{-}N_2)^+$ systems: implications for the neutralization of ionic molecular aggregates. Phys. Chem. Chem. Phys. **10**, 5993–6001 (2008). https://doi.org/10.1039/B808200F
28. Cappelletti, D., Pirani, F., Bussery-Honvault, B., Gomez, L., Bartolomei, M.: A bond-bond description of the intermolecular interaction energy: the case of weakly bound N_2-H_2 and N_2-N_2 complexes. Phys. Chem. Chem. Phys. **10**, 4281–4293 (2008). https://doi.org/10.1039/B803961E
29. Pacifici, L., Verdicchio, M., Faginas-Lago, N., Lombardi, A., Costantini, A.: A high-level ab initio study of the N_2 + N_2 reaction channel. J. Comput. Chem. **34**(31), 2668–2676 (2013). https://doi.org/10.1002/jcc.23415
30. Hanwell, M.D., Curtis, D.E., Lonie, D.C., Vandermeersch, T., Zurek, E., Hutchison, G.R.: Avogadro: an advanced semantic chemical editor, visualization, and analysis platform. J. Cheminform. **4**(1), 1–17 (2012)
31. Cernuto, A., Tosi, P., Martini, L.M., Pirani, F., Ascenzi, D.: Experimental investigation of the reaction of helium ions with dimethyl ether: stereodynamics of the dissociative charge exchange process. Phys. Chem. Chem. Phys. **19**(30), 19554–19565 (2017). https://doi.org/10.1039/C7CP00827A
32. Cernuto, A., Pirani, F., Martini, L.M., Tosi, P., Ascenzi, D.: The Selective Role of Long-Range Forces in the Stereodynamics of Ion-Molecule Reactions: the He^+ + Methyl Formate Case From Guided-Ion-Beam Experiments. Chem. Phys. Chem. **19**(1), 51–59 (2018). https://doi.org/10.1002/cphc.201701096
33. Richardson, V., et al.: Fragmentation of interstellar methanol by collisions with he+: an experimental and computational study. Phys. Chem. Chem. Phys. **24**(37), 22437–22452 (2022)